How to cite: *Angew. Chem. Int. Ed.* **2021**, *60*, 8683–8688
International Edition: doi.org/10.1002/anie.202015058
German Edition: doi.org/10.1002/ange.202015058

Quantum Bits Hot Paper

Blatter-Radical-Grafted Mesoporous Silica as Prospective Nanoplatform for Spin Manipulation at Ambient Conditions

Artem S. Poryvaev[+], Eva Gjuzi[+], Daniil M. Polyukhov, Frank Hoffmann, Michael Fröba, and Matvey V. Fedin**

Abstract: *Quantum computing and quantum information processing (QC/QIP) crucially depend on the availability of suitable quantum bits (qubits) and methods of their manipulation. Most qubit candidates known to date are not applicable at ambient conditions. Herein, we propose radical-grafted mesoporous silica as a versatile and prospective nanoplatform for spin-based QC/QIP. Extremely stable Blatter-type organic radicals are used, whose electron spin decoherence time is profoundly long even at room temperature (up to $T_m \approx 2.3$ μs), thus allowing efficient spin manipulation by microwave pulses. The mesoporous structure of such composites is nuclear-spin free and provides additional opportunities of embedding guest molecules into the channels. Robustness and tunability of these materials promotes them as highly promising nanoplatforms for future QC/QIP developments.*

Quantum technologies, including quantum computing (QC) and quantum information processing (QIP), are among the major hot topics of modern science, potentially leading humankind to a new technological revolution.[1–7] The implementations of QC/QIP protocols crucially depend on the availability and properties of individual quantum bits (qubits), and their development was an immense challenge for scientists over the past decade. Different types of qubits have been considered,[8–12] and spin-based ones have been intensively addressed as a promising route.[13–32] They were mainly represented by paramagnetic centers in silicon,[5,29] nitrogen vacancy (NV) and other centers in diamond,[26,27] SiC,[28] quantum dots,[30] semiconductors,[31,32] fullerenes,[15] paramagnetic metal complexes,[16–23,33] etc. However, each of these solutions has one or more drawbacks requiring further developments. For example, the paramagnetic metal complexes are versatile building blocks and allow construction of useful "spin architectures", for example, metal–organic frameworks (MOFs).[33] They can be very robust for applications; however, their electron spin decoherence time (or phase memory time, T_m) at room temperature is not optimal. In the record-setting vanadyl porphyrins it reaches $T_m \approx 1$ μs,[18–20] whereas longer T_m might be required for extensive QC/QIP protocols. The NV-centers in diamonds and paramagnetic centers in silicon manifest significantly higher T_m up to approximately 1 ms,[34,35] and they are very robust, but at the same they time lack tunability and control over their spatial arrangement at the nanoscale.[36]

Stable organic radicals and biradicals were also actively considered as promising qubit candidates for spin manipulation.[37,38] The weakness of this approach relates to still rather short relaxation times in the solid state at room temperature (typically $T_m < 1$ μs for nitroxides[39,40]) and insufficient stability for industrial applications. However, adjusting the structure of the radical moiety might remedy some of these problems; e.g., triarylmethyl (TAM) radicals feature T_m up to 2.2 μs in room-temperature solids.[41] Some organic radicals, similar to the metal complexes, can be assembled into functional architectures such as MOFs.[42] Therefore, pursuing the "radical approach" to spin qubits is quite promising.[43,44] Similar to other qubit candidates, it requires optimization of stability, increase of T_m, and development of strategies for mutual arrangement of the qubits.

Herein, we propose a new agenda to progress along the above-mentioned guidelines for developing room-temperature qubit systems. First of all, Blatter-type radicals are selected as spin-carrying blocks, whose tremendous stability over months to years at ambient conditions is well known,[45] but has not been thoroughly taken into account for the needs of QC/QIP up to date. Second, we efficiently embedded these radicals into well-defined mesoporous silica frameworks at suitable concentrations for spin manipulations. Such frameworks have drawn a lot of attention recently and were extensively used in various applications.[46–53] Finally, the room-temperature T_m values obtained using pulse electron paramagnetic resonance (EPR) were found >2 times higher than those achieved in metal complexes; they provided a sufficient time window to detect Rabi oscillations and thus perform quantum operations on electron spin. Below we

[*] A. S. Poryvaev,[+] D. M. Polyukhov, Prof. M. V. Fedin
International Tomography Center SB RAS
Novosibirsk, 630090 (Russia)
E-mail: mfedin@tomo.nsc.ru
E. Gjuzi,[+] Dr. F. Hoffmann, Prof. M. Fröba
Institute of Inorganic and Applied Chemistry
University of Hamburg
Martin-Luther-King-Platz 6, 20146 Hamburg (Germany)
E-mail: froeba@chemie.uni-hamburg.de
A. S. Poryvaev,[+] Prof. M. V. Fedin
Novosibirsk State University
Novosibirsk, 630090 (Russia)
[+] These authors contributed equally to this work.
Supporting information and the ORCID identification number(s) for the author(s) of this article can be found under: https://doi.org/10.1002/anie.202015058.

discuss this study in detail and outline additional benefits of incorporating spin blocks into mesoporous silica frameworks.

As mesoporous silica host material we used SBA-15 (Santa Barbara Amorphous-type material) samples with a two-dimensional hexagonal pore system and cylindrical pores with diameters of 9.1 nm. As a source of paramagnetic spin centers the Blatter-type bis(triethoxysilylvinyl)triazinyl radical (BTEV-BTR) precursor was used. After drying both powders for 18 hours in high vacuum, anhydrous toluene was added to SBA-15 with 20, 10, 5, 1, or 0% (reference) loading of the BTEV-BTR precursor (w/w, BTEV-BTR/SBA-15). First, the suspension was stirred for two hours at room temperature to ensure an even distribution of the precursor in the pores of the SBA-15 phase, followed by a heat treatment under reflux for 24 hours initiating the actual grafting procedure which leads to an immobilization of the radical moiety inside the pores of SBA-15 via condensation reaction (Figure 1); details are given in the Supporting Information (SI). Continuous-wave (CW) and pulse EPR measurements were performed using a commercial Bruker Elexsys E580 X/Q-band EPR spectrometer (see SI for details); simulations used EasySpin toolbox for Matlab.[54] If not mentioned otherwise, the samples were evacuated and sealed off in quartz sample tubes.

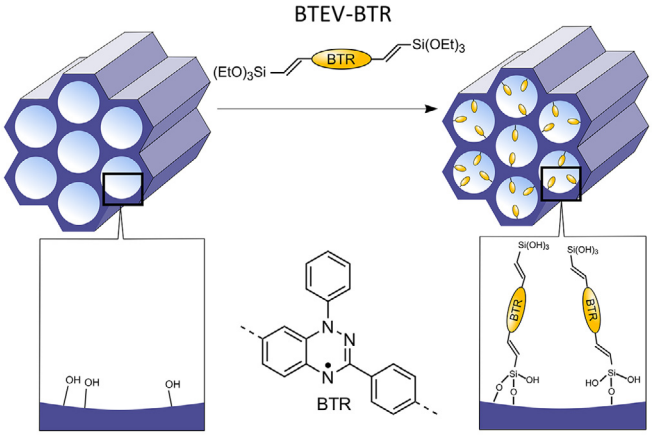

Figure 1. Schematic illustration of the grafting procedure leading to immobilized BTR radicals inside the pores of the SBA-15 host phase.

The amount of grafted radicals present in the product, quantified by thermogravimetric analysis (TGA) and CW EPR, was lower by a factor of 2–5 than the original load (see SI), but still very suitable for our study in all cases. Besides incomplete attachment, the deviations are due to mass losses caused by ethanol cleavage during condensation of the radical precursor to the silica matrix. Below we refer to original loadings for simplicity and label the compounds as R_{20}, R_{10}, R_5, R_1, and R_0, respectively.

Figure 2a shows the room-temperature CW EPR spectrum of the radical precursor dissolved in ethyl acetate, which can be sufficiently well simulated accounting for three ^{14}N nuclei with isotropic hyperfine interaction (HFI) constants $A_{iso,1} = 0.75$ mT, $A_{iso,2} = A_{iso,3} = 0.49$ mT. Such values agree well with the large amount of studies on various Blatter-

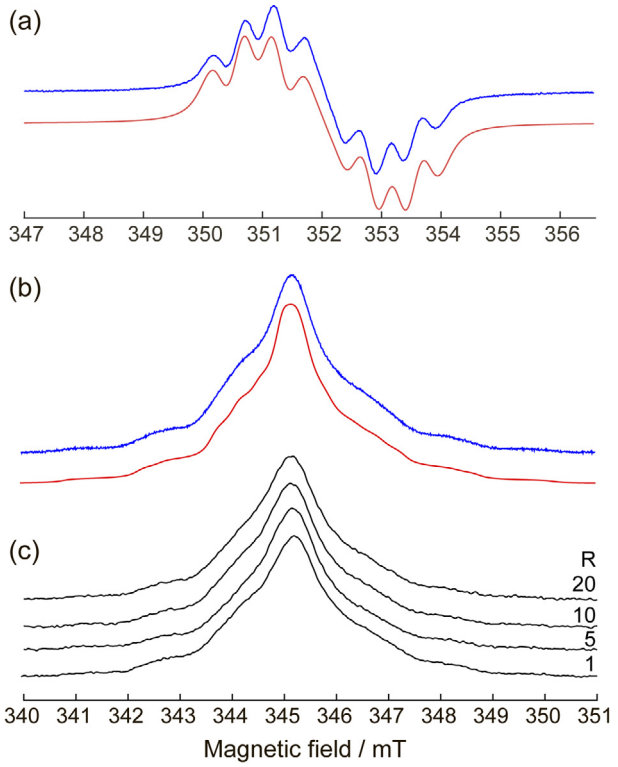

Figure 2. a) Experimental (blue) and simulated (red) CW EPR spectra of radical precursor (room temperature, ethyl acetate, see text for parameters). b) Experimental (blue) and simulated (red) FID-detected EPR spectra of radical in frozen toluene glass (80 K, see text for parameters). c) Experimental FID-detected EPR spectra of R_{20}–R_1 (indicated) at room temperature. All data were collected at X-band (9 GHz).

type radicals in solution.[45,55–57] However, anisotropic values of ^{14}N HFI constants for Blatter's radicals, which are needed for solid-state studies, have not been yet reported to the best of our knowledge. Figure 2b shows the X-band (9 GHz) free induction decay (FID)-detected EPR spectrum of a similar radical (used in our previous work,[42] see SI for details) recorded in frozen toluene glass (80 K). Simulations allow obtaining the corresponding HFI tensors $A_1 = [0.03\ 0.22\ 1.80]$ mT, $A_2 = A_3 = [0.01\ 0.01\ 1.38]$ mT and the g-tensor $g = [2.0043\ 2.0035\ 2.0015]$ (see Q-band data in SI). Minor imperfections of the fitting are due to the presence of many unresolved proton HFIs,[59] which cannot be taken into account rigorously in simulations.

Figure 2c shows a series of FID-detected EPR spectra of R_{20}–R_1 obtained at room temperature (Figure S27 shows the corresponding CW EPR spectra), which are all similar to the low-temperature spectrum of the dissolved radical (Figure 2b).

In order to evaluate the suitability of R_1–R_{20} as room-temperature qubits, their transverse and longitudinal electron spin relaxation times (T_m and T_1, respectively) were first measured at 298 K in the global maximum of the spectrum, see Table 1. The joint trend of decreasing T_1 and T_m with an increase of radical concentration is observed, meaning that spin–spin interactions between radicals play a profound role in the overall relaxation. The trend is approximately linear for

Table 1: Room-temperature relaxation times for R_1–R_{20}. The accuracy is 0.5 µs for T_1 and 0.01 µs for T_m.

Radical [%]	T_1 [µs]	T_m [µs]
1	36	2.30
5	29	1.73
10	26	1.43
20	20	0.98

both T_1 and T_m, without any signs of approaching a plateau; therefore, relaxation can be further prolonged by using yet smaller radical loadings. However, even in the current settings, the room-temperature $T_m = 2.30 \pm 0.01$ µs obtained for R_1 is the record-setting one, being significantly longer than that of the vanadyl qubits ($T_m \approx 1$ µs[18,19]), and even slightly exceeding that for the TAM radical in glassy trehalose ($T_m =$ 2.2 µs[41]).

Figure 3 shows the temperature dependence of representative T_m and T_1 for the most concentrated (R_{20}) and least concentrated (R_1) samples in the series. Both relaxations for R_{20} show weak temperature dependence, implying that the concentration-induced contribution is the decisive one. In case of R_1 a noticeable enhancement of T_1 is observed at low temperatures, whereas T_m is only moderately increased. Therefore, compared to other qubits, for example, vanadyl-based ones, the advantage of Blatter-radical-grafted SBA materials is manifested at ambient temperatures, which are most relevant for prospective applications.

The shape of the EPR spectrum is quite complex, owing to the presence of three appreciable ^{14}N HFI constants and many smaller (unresolved) proton ones. In case of vanadyl qubits the superior T_m values were obtained at the shoulder of the EPR spectrum (not at its global maximum); therefore, a trade-off between the signal intensity and higher T_m values had to be pursued. This motivated us to investigate the T_m across the EPR spectrum in R_1–R_{20} materials as well. Figure 4a presents T_m vs. magnetic field, and Figure 4b shows the 3D plot of the echo signal intensity vs. time and vs. magnetic field for R_5 (representative). Evidently, the longest echo decay T_m is observed at the global maximum. Therefore, in case of Blatter-radical-decorated SBA materials the signal intensity does not need to be sacrificed for the sake of longer T_m, and performing quantum operations at global maximum is the optimum choice.

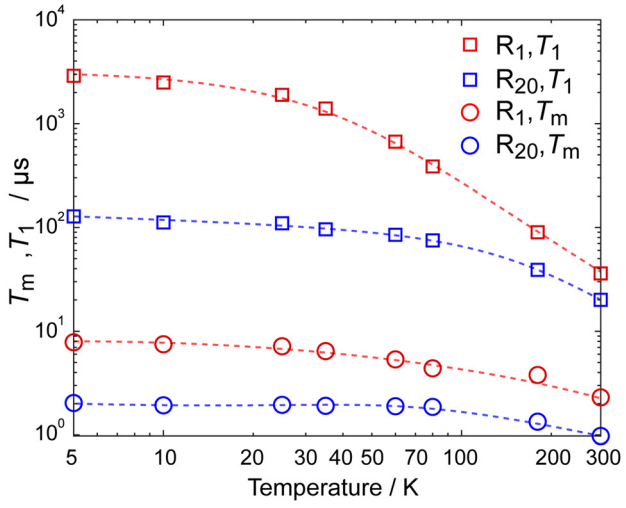

Figure 3. Relaxation times T_m and T_1 vs. temperature measured for R_{20} and R_1. The lines guide the eye. See Table S4 for the tabulated values of relaxation times.

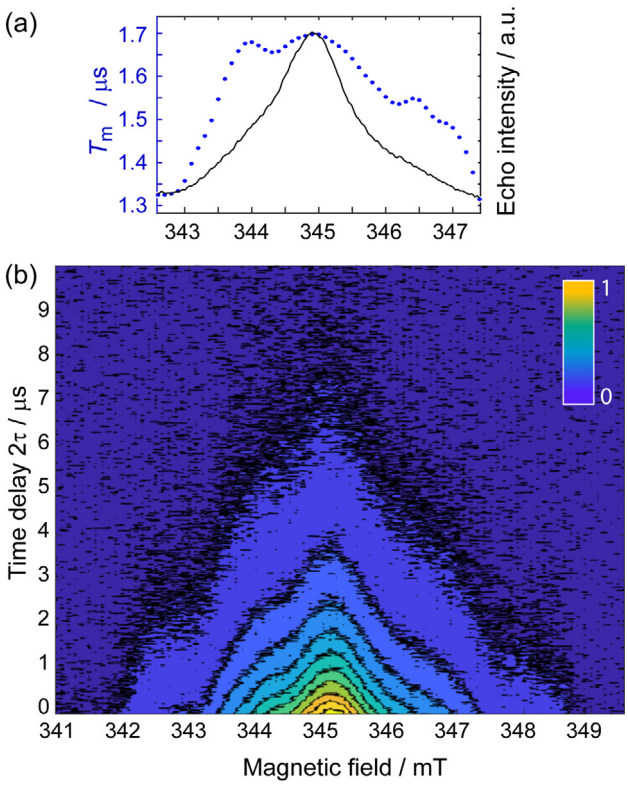

Figure 4. Relaxation measurements for representative R_5 at room temperature. a) Magnetic field dependence of T_m (blue circles, left axis) overlaid with the corresponding echo-detected EPR spectrum (black). The accuracy of T_m is 0.01 µs. b) Two-pulse echo intensity (given by color map) plotted vs. magnetic field and interpulse delay τ.

The porous structure of radical-decorated SBA materials provides additional ways to modify their functionalities and combine them with the qubit functions by embedding guest molecules and exploiting host–guest interactions and molecular sieving properties. To avoid shortening of the relaxation times, nuclear spin-free guests are preferred, because filling of the channels with, for example, proton-carrying molecules would expectedly lead to the shortening of the relaxation due to the nuclear spin diffusion. Table S5 shows how the T_m value changes when the channels are filled with guest molecules such as *o*-terphenyl or sulfur. We envision that carrying out the target reactions (e.g. complexation) with radicals would not lead to profound nuclear spin diffusion and can be considered as a future route for creating more complex structures based on the grafted radicals.

Finally, we demonstrate that quantum operations at room temperature can successfully be performed using a simplest nutation (Rabi oscillation) experiment.[13] In this experiment electron magnetization is flipped by a single microwave (mw)

pulse of variable length t_p, which is then detected in our case by the FID integral (see SI for details). Strictly speaking, spin states of ^{14}N nuclei are also involved; in the future they can either be used within such electron–nuclear qudits, or can be neglected if electron–electron couplings between neighboring qubits are targeted for entanglement. Figure 5a shows that many oscillations (nutations) of electron magnetization can be obtained, where each full period corresponds to the complete turnover of magnetization by 360°. The experiments at several values of microwave power attenuation show that the frequency of oscillations (see Fourier-transform in Figure 5b) is linearly dependent on the magnitude of the mw field (Figure 5c), thus confirming the feasibility of spin manipulation.

In summary, we have proposed Blatter-radical-grafted mesoporous silica materials (exemplified with SBA-15) as prospective platforms for the realization of spin qubits. There are several crucial advantages of this new strategy, namely:

(i) The observed electron spin decoherence (phase memory) time T_m is sufficiently long to provide a time window for quantum operations at ambient conditions (room temperature). $T_m = 2.3$ µs was obtained for the most dilute sample, and the trend in the series assumes possibilities for a further increase of T_m; however, a reasonable compromise between signal intensity and the T_m value should be considered. The value $T_m = 2.3$ µs is more than two times higher compared to vanadyl qubits and is slightly higher compared to slow-relaxing radicals like TAM. The profoundly long T_m is ascribed to the nature of the Blatter radical and, more important, nuclear spin-free composition of SBA-15 material. The only magnetic nuclei around the electron spin are the radical's own protons and nitrogen atoms, and the protons can be replaced by deuterons[58] to enhance T_m further. Some narrowing of the spectrum, if needed, can be achieved by using ^{15}N-labeled radicals.

(ii) The Blatter-type radicals are known to be extremely stable,[45] which is favorable for potential QC/QIP implementations at ambient conditions and was not carefully attended before. We assume that a mesoporous silica host might act as additional protector and stabilizer of these radicals against reducing agents and aggressive surroundings.

(iii) The mesoporous structure of the studied organosilica phases opens up new possibilities to influence electron spins by embedding guest molecules into the channels and, more intriguing, designing new spin structures by means of added guest molecules.

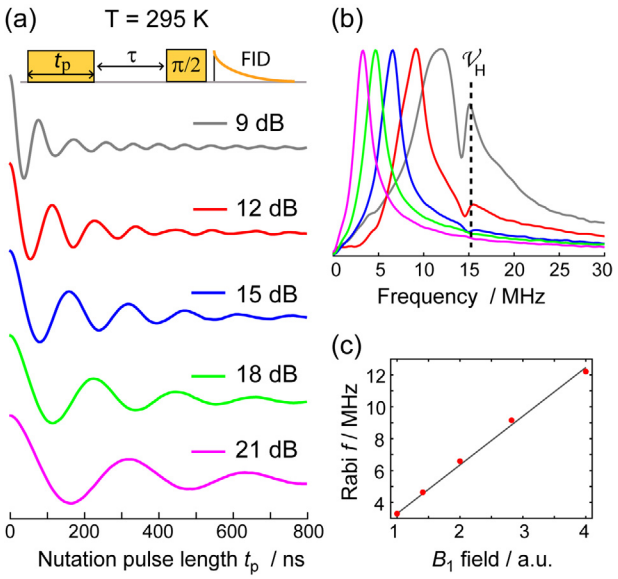

Figure 5. Representative quantum manipulation experiment on R_5 at room temperature. a) Top: pulse sequence used (details in SI). Rabi oscillations measured at five values of mw power P (expressed by attenuation in dB units). The mw field B_1 is proportional to the $\sqrt{P}$. b) Fourier-transform spectra of data shown in (a); ν_H-peak arises due to weak electron–nuclear interactions (ESEEM) with the own protons of the radical and vanishes at smaller P values (i.e. higher dB). c) Rabi frequency f vs. normalized amplitude of B_1 field.

Apart from the long electron decoherence time and spin manipulation by mw pulses, the development of room-temperature qubits requires scalability, initialization, and individual addressing. Synthetic strategies for entanglement of neighboring qubits via loading of prearranged structures or creating arrays of attached radicals with controlled separation still need to be developed; however, some promising routes for organosilica have been already reported.[59,60] Both initialization and individual addressing can potentially be performed by a transfer of spin hyperpolarization from photoexcited triplet molecules (e.g. porphyrins or fullerenes, either guests in the channels or covalently linked to the radical). Of course, the real potential of these strategies was not yet explored in the present work and might be a fruitful topic for future investigations.

Overall, the present study offers an outlook on many promising directions for the realization of qubits for QC/QIP on the basis of multifunctional, robust, and tuneable Blatter-radical-grafted mesoporous silica.

Acknowledgements

This work was funded by RFBR (No 20-53-12005) and the Deutsche Forschungsgemeinschaft (DFG, German Research Foundation)—Projektnummer 429839772 in a DFG-RFBR collaborative project. We thank the Ministry of Science and Higher Education (MSHE) of the Russian Federation for access to the EPR equipment. We thank Natascha Speil for provision of SBA-15 test samples and synthesis specification. Open access funding enabled and organized by Projekt DEAL.

Conflict of interest

The authors declare no conflict of interest.

Keywords: EPR spectroscopy · mesoporous materials · mesoporous organosilica · qubits · radicals

[1] D. P. DiVincenzo, *Science* **1995**, *270*, 255.
[2] S. J. Glaser, *Angew. Chem. Int. Ed.* **2001**, *40*, 147 – 149; *Angew. Chem.* **2001**, *113*, 151 – 153.
[3] T. D. Ladd, F. Jelezko, R. Laflamme, Y. Nakamura, C. Monroe, J. L. O'Brien, *Nature* **2010**, *464*, 45 – 53.
[4] M. A. Nielsen, I. Chuang, L. K. Grover, *Am. J. Phys.* **2002**, *70*, 558 – 559.
[5] J. J. Pla, K. Y. Tan, J. P. Dehollain, W. H. Lim, J. J. L. Morton, D. N. Jamieson, A. S. Dzurak, A. Morello, *Nature* **2012**, *489*, 541 – 544.
[6] M. Warner, S. Din, I. S. Tupitsyn, G. W. Morley, A. M. Stoneham, J. A. Gardener, Z. Wu, A. J. Fisher, S. Heutz, C. W. M. Kay, G. Aeppli, *Nature* **2013**, *503*, 504 – 508.
[7] M. Atzori, R. Sessoli, *J. Am. Chem. Soc.* **2019**, *141*, 11339 – 11352.
[8] E. Knill, R. Laflamme, G. J. Milburn, *Nature* **2001**, *409*, 46 – 52.
[9] H. Pichler, S. Choi, P. Zoller, M. D. Lukin, *Proc. Natl. Acad. Sci. USA* **2017**, *114*, 11362 – 11367.
[10] X. Qiang, X. Zhou, J. Wang, C. M. Wilkes, T. Loke, S. O'Gara, L. Kling, G. D. Marshall, R. Santagati, T. C. Ralph, J. B. Wang, J. L. O'Brien, M. G. Thompson, J. C. F. Matthews, *Nat. Photonics* **2018**, *12*, 534 – 539.
[11] Y. Nakamura, Y. A. Pashkin, J. S. Tsai, *Nature* **1999**, *398*, 786 – 788.
[12] B. Lucatto, D. S. Koda, F. Bechstedt, M. Marques, L. K. Teles, *Phys. Rev. B* **2019**, *100*, 121406.
[13] M. Affronte, I. Casson, M. Evangelisti, A. Candini, S. Carretta, C. A. Muryn, S. J. Teat, G. A. Timco, W. Wernsdorfer, R. E. P. Winpenny, *Angew. Chem. Int. Ed.* **2005**, *44*, 6496 – 6500; *Angew. Chem.* **2005**, *117*, 6654 – 6658.
[14] L. M. K. Vandersypen, M. Breyta, G. Steffen, C. S. Yannoni, M. H. Sherwood, I. L. Chuang, *Nature* **2001**, *414*, 883 – 887.
[15] J. J. L. Morton, A. M. Tyryshkin, A. Ardavan, S. C. Benjamin, K. Porfyrakis, S. A. Lyon, G. A. D. Briggs, *Nat. Phys.* **2006**, *2*, 40 – 43.
[16] G. A. Timco, S. Carretta, F. Troiani, F. Tuna, R. J. Pritchard, C. A. Muryn, E. J. L. McInnes, A. Ghirri, A. Candini, P. Santini, G. Amoretti, M. Affronte, R. E. P. Winpenny, *Nat. Nanotechnol.* **2009**, *4*, 173 – 178.
[17] C. J. Wedge, G. A. Timco, E. T. Spielberg, R. E. George, F. Tuna, S. Rigby, E. J. L. McInnes, R. E. P. Winpenny, S. J. Blundell, A. Ardavan, *Phys. Rev. Lett.* **2012**, *108*, 107204.
[18] M. Atzori, L. Tesi, E. Morra, M. Chiesa, L. Sorace, R. Sessoli, *J. Am. Chem. Soc.* **2016**, *138*, 2154 – 2157.
[19] M. Atzori, E. Morra, L. Tesi, A. Albino, M. Chiesa, L. Sorace, R. Sessoli, *J. Am. Chem. Soc.* **2016**, *138*, 11234 – 11244.
[20] M. Atzori, L. Tesi, S. Benci, A. Lunghi, R. Righini, A. Taschin, R. Torre, L. Sorace, R. Sessoli, *J. Am. Chem. Soc.* **2017**, *139*, 4338 – 4341.
[21] J. M. Zadrozny, J. Niklas, O. G. Poluektov, D. E. Freedman, *J. Am. Chem. Soc.* **2014**, *136*, 15841 – 15844.
[22] J. M. Zadrozny, J. Niklas, O. G. Poluektov, D. E. Freedman, *ACS Cent. Sci.* **2015**, *1*, 488 – 492.
[23] C. J. Yu, M. J. Graham, J. M. Zadrozny, J. Niklas, M. D. Krzyaniak, M. R. Wasielewski, O. G. Poluektov, D. E. Freedman, *J. Am. Chem. Soc.* **2016**, *138*, 14678 – 14685.
[24] K. Sato, S. Nakazawa, R. Rahimi, T. Ise, S. Nishida, T. Yoshino, N. Mori, K. Toyota, D. Shiomi, Y. Yakiyama, Y. Morita, M. Kitagawa, K. Nakasuji, M. Nakahara, H. Hara, P. Carl, P. Höfer, T. Takui, *J. Mater. Chem.* **2009**, *19*, 3739 – 3754.
[25] M. Zhong, M. P. Hedges, R. L. Ahlefeldt, J. G. Bartholomew, S. E. Beavan, S. M. Wittig, J. J. Longdell, M. J. Sellars, *Nature* **2015**, *517*, 177 – 180.
[26] F. Jelezko, T. Gaebel, I. Popa, A. Gruber, J. Wrachtrup, *Phys. Rev. Lett.* **2004**, *92*, 076401.
[27] M. V. Gurudev Dutt, L. Childress, L. Jiang, E. Togan, J. Maze, F. Jelezko, A. S. Zibrov, P. R. Hemmer, M. D. Lukin, *Science* **2007**, *316*, 1312 – 1316.
[28] D. J. Christle, A. L. Falk, P. Andrich, P. V. Klimov, J. U. Hassan, N. T. Son, E. Janzén, T. Ohshima, D. D. Awschalom, *Nat. Mater.* **2015**, *14*, 160 – 163.
[29] J. J. L. Morton, D. R. McCamey, M. A. Eriksson, S. A. Lyon, *Nature* **2011**, *479*, 345 – 353.
[30] M. Veldhorst, J. C. C. Hwang, C. H. Yang, A. W. Leenstra, B. De Ronde, J. P. Dehollain, J. T. Muhonen, F. E. Hudson, K. M. Itoh, A. Morello, A. S. Dzurak, *Nat. Nanotechnol.* **2014**, *9*, 981 – 985.
[31] J. R. Petta, A. C. Johnson, J. M. Taylor, E. A. Laird, A. Yacoby, M. D. Lukin, C. M. Marcus, M. P. Hanson, A. C. Gossard, *Science* **2005**, *309*, 2180 – 2184.
[32] J. Tribollet, J. Behrends, K. Lips, *EPL* **2008**, *84*, 20009.
[33] T. Yamabayashi, M. Atzori, L. Tesi, G. Cosquer, F. Santanni, M. E. Boulon, E. Morra, S. Benci, R. Torre, M. Chiesa, L. Sorace, R. Sessoli, M. Yamashita, *J. Am. Chem. Soc.* **2018**, *140*, 12090 – 12101.
[34] G. Balasubramanian, P. Neumann, D. Twitchen, M. Markham, R. Kolesov, N. Mizuochi, J. Isoya, J. Achard, J. Beck, J. Tissler, V. Jacques, P. R. Hemmer, F. Jelezko, J. Wrachtrup, *Nat. Mater.* **2009**, *8*, 383 – 387.
[35] M. Widmann, S. Y. Lee, T. Rendler, N. T. Son, H. Fedder, S. Paik, L. P. Yang, N. Zhao, S. Yang, I. Booker, A. Denisenko, M. Jamali, S. Ali Momenzadeh, I. Gerhardt, T. Ohshima, A. Gali, E. Janzén, J. Wrachtrup, *Nat. Mater.* **2015**, *14*, 164 – 168.
[36] D. McCloskey, D. Fox, N. O'Hara, V. Usov, D. Scanlan, N. McEvoy, G. S. Duesberg, G. L. W. Cross, H. Z. Zhang, J. F. Donegan, *Appl. Phys. Lett.* **2014**, *104*, 031109.
[37] S. Nakazawa, S. Nishida, T. Ise, T. Yoshino, N. Mori, R. D. Rahimi, K. Sato, Y. Morita, K. Toyota, D. Shiomi, M. Kitagawa, H. Hara, P. Carl, P. Höfer, T. Takui, *Angew. Chem. Int. Ed.* **2012**, *51*, 9860 – 9864; *Angew. Chem.* **2012**, *124*, 9998 – 10002.
[38] K. Sugisaki, S. Nakazawa, K. Toyota, K. Sato, D. Shiomi, T. Takui, *ACS Cent. Sci.* **2019**, *5*, 167 – 175.
[39] A. A. Kuzhelev, R. K. Strizhakov, O. A. Krumkacheva, Y. F. Polienko, D. A. Morozov, G. Y. Shevelev, D. V. Pyshnyi, I. A. Kirilyuk, M. V. Fedin, E. G. Bagryanskaya, *J. Magn. Reson.* **2016**, *266*, 1 – 7.
[40] V. Meyer, M. A. Swanson, L. J. Clouston, P. J. Boratyński, R. A. Stein, H. S. McHaourab, A. Rajca, S. S. Eaton, G. R. Eaton, *Biophys. J.* **2015**, *108*, 1213 – 1219.
[41] A. A. Kuzhelev, G. Y. Shevelev, O. A. Krumkacheva, V. M. Tormyshev, D. V. Pyshnyi, M. V. Fedin, E. G. Bagryanskaya, *J. Phys. Chem. Lett.* **2016**, *7*, 2544 – 2548.
[42] A. S. Poryvaev, D. M. Polyukhov, E. Gjuzi, F. Hoffmann, M. Fröba, M. V. Fedin, *Inorg. Chem.* **2019**, *58*, 8471 – 8479.
[43] J. McGuire, H. N. Miras, E. Richards, S. Sproules, *Chem. Sci.* **2019**, *10*, 1483 – 1491.
[44] M. Mas-Torrent, N. Crivillers, C. Rovira, J. Veciana, *Chem. Rev.* **2012**, *112*, 2506 – 2527.
[45] C. P. Constantinides, P. A. Koutentis, H. Krassos, J. M. Rawson, A. J. Tasiopoulos, *J. Org. Chem.* **2011**, *76*, 2798 – 2806.
[46] S. Che, K. Lund, T. Tatsumi, S. Iijima, S. H. Joo, R. Ryoo, O. Terasaki, *Angew. Chem. Int. Ed.* **2003**, *42*, 2182 – 2185; *Angew. Chem.* **2003**, *115*, 2232 – 2235.
[47] J. Fan, C. Yu, F. Gao, J. Lei, B. Tian, L. Wang, Q. Luo, B. Tu, W. Zhou, D. Zhao, *Angew. Chem. Int. Ed.* **2003**, *42*, 3146 – 3150; *Angew. Chem.* **2003**, *115*, 3254 – 3258.
[48] V. Rebbin, R. Schmidt, M. Fröba, *Angew. Chem. Int. Ed.* **2006**, *45*, 5210 – 5214; *Angew. Chem.* **2006**, *118*, 5335 – 5339.
[49] B. Karimi, S. Abedi, J. H. Clark, V. Budarin, *Angew. Chem. Int. Ed.* **2006**, *45*, 4776 – 4779; *Angew. Chem.* **2006**, *118*, 4894 – 4897.
[50] R. K. Zeidan, S.-J. Hwang, M. E. Davis, *Angew. Chem. Int. Ed.* **2006**, *45*, 6332 – 6335; *Angew. Chem.* **2006**, *118*, 6480 – 6483.

[51] S. Hudson, J. Cooney, E. Magner, *Angew. Chem. Int. Ed.* **2008**, *47*, 8582 – 8594; *Angew. Chem.* **2008**, *120*, 8710 – 8723.
[52] S. Inagaki, O. Ohtani, Y. Goto, K. Okamoto, M. Ikai, K. Yamanaka, T. Tani, T. Okada, *Angew. Chem. Int. Ed.* **2009**, *48*, 4042 – 4046; *Angew. Chem.* **2009**, *121*, 4102 – 4106.
[53] J. B. Mietner, F. J. Brieler, Y. J. Lee, M. Fröba, *Angew. Chem. Int. Ed.* **2017**, *56*, 12348 – 12351; *Angew. Chem.* **2017**, *129*, 12519 – 12523.
[54] S. Stoll, A. Schweiger, *J. Magn. Reson.* **2006**, *178*, 42 – 55.
[55] Y. Ji, L. Long, Y. Zheng, *Mater. Chem. Front.* **2020**, *4*, 3433 – 3443.
[56] P. Bartos, B. Anand, A. Pietrzak, P. Kaszyński, *Org. Lett.* **2020**, *22*, 180 – 184.
[57] N. M. Gallagher, J. J. Bauer, M. Pink, S. Rajca, A. Rajca, *J. Am. Chem. Soc.* **2016**, *138*, 9377 – 9380.
[58] F. A. Neugebauer, G. Rimmler, *Magn. Reson. Chem.* **1988**, *26*, 595 – 600.
[59] L. Grösch, Y. J. Lee, F. Hoffmann, M. Fröba, *Chem. Eur. J.* **2015**, *21*, 331 – 346.
[60] M. Beretta, J. Morell, P. Sozzani, M. Fröba, *Chem. Commun.* **2010**, *46*, 2495 – 2497.

Manuscript received: November 11, 2020
Revised manuscript received: January 11, 2021
Accepted manuscript online: January 24, 2021
Version of record online: March 9, 2021

